Acta Crystallographica Section D
Biological Crystallography
ISSN 0907-4449

Structure of fully liganded Hb $\zeta_2\beta_2^s$ trapped in a tense conformation

Martin K. Safo,[a]* Tzu-Ping Ko,[b] Osheiza Abdulmalik,[c] Zhenning He,[d] Andrew H.-J. Wang,[b] Eric R. Schreiter[e] and J. Eric Russell[c,d]*

[a]Institute for Structural Biology and Drug Discovery, and the Department of Medicinal Chemistry, School of Pharmacy, Virginia Commonwealth University, Richmond, VA 23298, USA, [b]Institute of Biological Chemistry, Academia Sinica, Taipei 11529, Taiwan, [c]Division of Hematology, The Children's Hospital of Philadelphia, Philadelphia, PA 19104, USA, [d]Division of Hematology–Oncology, Perelman School of Medicine at the University of Pennsylvania, Philadelphia, PA 19104, USA, and [e]Howard Hughes Medical Institute, Janelia Farm Research Campus, Ashburn, VA 20147, USA

Correspondence e-mail: msafo@vcu.edu, jeruss@mail.med.upenn.edu

Received 6 June 2013
Accepted 10 July 2013

PDB Reference: Hb $\zeta_2\beta_2^s$, 3w4u

A variant Hb $\zeta_2\beta_2^s$ that is formed from sickle hemoglobin (Hb S; $\alpha_2\beta_2^s$) by exchanging adult α-globin with embryonic ζ-globin subunits shows promise as a therapeutic agent for sickle-cell disease (SCD). Hb $\zeta_2\beta_2^s$ inhibits the polymerization of deoxygenated Hb S *in vitro* and reverses characteristic features of SCD *in vivo* in mouse models of the disorder. When compared with either Hb S or with normal human adult Hb A ($\alpha_2\beta_2$), Hb $\zeta_2\beta_2^s$ exhibits atypical properties that include a high oxygen affinity, reduced cooperativity, a weak Bohr effect and blunted 2,3-diphosphoglycerate allostery. Here, the 1.95 Å resolution crystal structure of human Hb $\zeta_2\beta_2^s$ that was expressed in complex transgenic knockout mice and purified from their erythrocytes is presented. When fully liganded with carbon monoxide, Hb $\zeta_2\beta_2^s$ displays a central water cavity, a $\zeta1$–β^s2 (or $\zeta2$–β^s1) interface, intersubunit salt-bridge/hydrogen-bond interactions, C-terminal βHis146 salt-bridge interactions, and a β-cleft, that are highly unusual for a relaxed hemoglobin structure and are more typical of a tense conformation. These quaternary tense-like features contrast with the tertiary relaxed-like conformations of the $\zeta1\beta^s1$ dimer and the CD and FG corners, as well as the overall structures of the heme cavities. This crystallographic study provides insights into the altered oxygen-transport properties of Hb $\zeta_2\beta_2^s$ and, moreover, decouples tertiary- and quaternary-structural events that are critical to Hb ligand binding and allosteric function.

1. Introduction

The principal physiological function of hemoglobin (Hb) is to bind oxygen in the lungs and to subsequently release it to metabolically active tissues. Functional hemoglobins are heterotetrameric in form, comprising four monomeric globin subunits, each encompassing an iron-containing protoporphyrin prosthesis capable of binding O_2 or any of several other gaseous ligands. Human adult hemoglobin (Hb A; $\alpha_2\beta_2$), which comprises $\alpha1\beta1$ and $\alpha2\beta2$ heterodimers surrounding a central water cavity, exists in equilibrium between two tetrameric conformations: the tense (T) state and the relaxed (R) state (Perutz, 1972*a*,*b*). The T and R conformations exhibit low and high affinities for ligand, respectively, providing a structural basis for cooperative effects that facilitate the efficient uptake and release of O_2 *in vivo*.

The low oxygen affinity of T-state heterotetramers has been attributed, in part, to events that alter the tertiary arrangement of the heme environment, including the positions of the central Fe^{2+} and elements of the E helix, C helix, F helix, CD corner and FG corner that encompass it. Each of these globin segments (except for the E helix) also contributes to the $\alpha1$–$\beta2$ ($\alpha2$–$\beta1$) dimer interface; consequently, changes to the structure of the heme cavity are also manifested at the dimer

interface. For example, tension in the Fe^{2+}–His(F8) bond restrains unliganded heme iron from moving into the plane of the porphyrin ring (Perutz, 1972*b*; Perutz *et al.*, 1998; Paoli *et al.*, 1997). Upon binding by O_2, the iron is displaced into the porphyrin plane, inducing conformational changes to the globin CD and FG corners that extend to the $\alpha1$–$\beta2$ ($\alpha2$–$\beta1$) dimer interface and, subsequently, trigger cooperativity events that effect the T→R transition (Perutz, 1972*b*; Perutz *et al.*, 1998; Paoli *et al.*, 1997; Baldwin & Chothia, 1979). Similarly, a shift in the position of the β-subunit E helix from the heme pocket upon ligand binding increases the size of the distal pocket and reduces steric contacts between the ligand and the E-helix residues βVal67 and βHis63, resulting in an increase in heme affinity for ligand (Perutz, 1972*b*, 1989; Perutz *et al.*, 1998; Paoli *et al.*, 1997).

The ligand affinity of most mammalian hemoglobins is dependent upon the ambient pH (the Bohr effect), a property that arises in part from tertiary-structural perturbations within the quaternary structure (Yonetani *et al.*, 2002; Yonetani & Tsuneshige, 2003; Shibayama & Saigo, 2001) and in part by effects on the equilibrium between the quaternary T and R structures (Perutz *et al.*, 1998; Perutz, 1972*a*,*b*). The C-terminal residues of both the α and β chains (αArg141 and βHis146, respectively) have been mechanistically implicated in the Bohr effect, which facilitates the release of Hb-bound O_2 in metabolically active environments (Perutz *et al.*, 1993, 1994, 1998; Perutz, 1976; O'Donnell *et al.*, 1979; Bettati *et al.*, 1997, 1998; Kavanaugh, Rogers & Arnone, 1992; Mozzarelli *et al.*, 1991). At acidic pH values, protonated β1His146 participates in a salt-bridge interaction with the carboxyl of β1Asp94 and the amine of α2Lys40 that stabilizes the low-affinity T structure and consequently facilitates O_2 release. Under similar conditions of pH, the C-terminal α1Arg141 makes separate salt-bridge interactions with the amine of α2Lys127 and the carboxyl of α2Asp126, further stabilizing the T-state structure. Protonated α1Arg141 also participates in a chloride-mediated interaction with the N-terminal α2Val1 that supplements this effect (Perutz, 1976; O'Donnell *et al.*, 1979; Perutz *et al.*, 1994; Fermi, 1975; Kavanaugh, Rogers, Case *et al.*, 1992; Kavanaugh *et al.*, 1995). At higher pH values all of these salt-bridge interactions are broken, which increases the mobility of both αArg141 and βHis146 and shifts the allosteric equilibrium towards the R state, thereby effecting a concomitant increase in Hb oxygen affinity.

Both hemoglobin cooperativity and allostery can be manifested through heterotropic effects within a single quaternary state (Bettati & Mozzarelli, 1997; Bruno *et al.*, 2001; Yonetani *et al.*, 2002; Yonetani & Tsuneshige, 2003; Shibayama & Saigo, 2001) as well as by quaternary changes to the heterotetramer structure that define the T→R transition (Perutz, 1972*b*, 1989; Perutz *et al.*, 1998). The latter process, which is characterized by rotation of the $\alpha1\beta1$ dimer relative to the $\alpha2\beta2$ dimer, significantly reshapes the $\alpha1$–$\beta2$ ($\alpha2$–$\beta1$), $\alpha1$–$\alpha2$ and $\beta1$–$\beta2$ dimer interfaces. For instance, the T and R structures of Hb A differ by a one and one-half turn in the FG corner β1His97 residue, a component of the $\alpha2$–$\beta1$ ($\alpha1$–$\beta2$) interface, that displaces it from between α2Pro44 and α2Thr41 in the T structure to between α2Thr41 and α2Thr38 in the R structure (Baldwin & Chothia, 1979). As might be anticipated, the relative rotation of the two $\alpha\beta$ heterodimers also alters the hydrogen-bond/salt-bridge interactions across the $\alpha1$–$\beta2$, $\beta1$–$\beta2$ and $\alpha1$–$\alpha2$ interfaces, the volume of the central water cavity that they surround and the sizes of the clefts defined by the two α (α-cleft) and β (β-cleft) subunits.

The classical T-state and R-state quaternary structures were originally determined and subsequently embodied in the Monod–Wyman–Changeux (MWC) allosteric model (Monod *et al.*, 1965). Since that time, additional species have been identified that exhibit explicit high-affinity tertiary R-like ('r') or low-affinity tertiary T-like ('t') conformations within the quaternary T and R states (Henry *et al.*, 2002; Eaton *et al.*, 2007; Viappiani *et al.*, 2004), as well as quaternary relaxed states (R2, R3, RR2, RR3 *etc.*) that extend beyond the classical T→R transition (Safo *et al.*, 2011; Jenkins *et al.*, 2009; Safo & Abraham, 2005; Mueser *et al.*, 2000; Silva *et al.*, 1992; Lukin *et al.*, 2003; Schumacher *et al.*, 1995, 1997; Janin & Wodak, 1993). Subsequent allosteric models have been proposed to resolve the limitations of the original MWC construct (Szabo & Karplus, 1972; Lee & Karplus, 1983; Henry *et al.*, 2002; Yonetani & Tsuneshige, 2003), including a tertiary two-state model that accounts for the high- and low-affinity r and t conformations, respectively, that are observed to occur in both the T and R quaternary structures (Henry *et al.*, 2002; Eaton *et al.*, 2007; Viappiani *et al.*, 2004). Each of these models, though, maintains the original MWC tenet that cooperative oxygen binding cannot occur in the absence of quaternary transition (Henry *et al.*, 2002), consistent with the fact that a fully liganded T-state hemoglobin heterotetramer obtained from ligated hemoglobin in solution has never been reported.

Hb S ($\alpha_2\beta_2^s$) is a variant hemoglobin comprising a Glu→Val substitution at β-globin position 6 that facilitates pathological self-assembly of the deoxygenated heterotetramers. Conditions that slow or prevent polymerization of deoxyHb S can mitigate the phenotype of sickle-cell disease (SCD) in individuals who express large amounts of this abnormal hemoglobin. One common therapeutic strategy for SCD involves the exchange of either the α or the β^s subunits for structurally related, developmentally silenced globin monomers that efficiently exclude the modified heterotetramer from pathological deoxyHb aggregates. One such variant, Hb $\zeta_2\beta_2^s$, is assembled by combining β^s-globin subunits and developmentally silenced α-like embryonic ζ-globin subunits (He & Russell, 2002, 2004*a*,*b*) that are identical at 83 of 141 amino-acid residues (Bunn & Forget, 1986). The pathological phenotype is effectively normalized in mouse models of SCD that are engineered to co-express a small amount of ζ globin, suggesting a novel approach for treating the corresponding human disorder (He & Russell, 2004*a*,*b*). Although therapeutically promising, Hb $\zeta_2\beta_2^s$ exhibits ligand-binding properties that differ from both Hb A and Hb S, including a markedly increased oxygen affinity (P_{50} values of 263, 511 and 401 Pa for Hb $\zeta_2\beta_2^s$, Hb A and Hb S, respectively), low subunit cooperativity {$\log[(Y/(1-Y)]/\log PO_2$ = 1.87, 2.84 and 2.81, respectively}, a reduced Bohr effect ($\Delta\log P_{50}/\Delta$pH = −0.21, −0.51 and −0.53,

Table 1
Data-collection and refinement statistics for Hb $\zeta_2\beta_2^s$.

Values in parentheses are for the highest resolution shell. All positive reflections were used in the refinement.

Data collection	
Space group	$P3_121$
Unit-cell parameters (Å)	$a = b = 115.5$, $c = 140.9$
Resolution (Å)	19.95–1.95 (2.02–1.95)
Unique reflections	79112 (7883)
Multiplicity	13.4 (4.0)
Completeness (%)	99.5 (98.7)
Average $I/\sigma(I)$	17.6 (2.4)
R_{merge}† (%)	7.9 (41.5)
Refinement	
No. of reflections	73114 (6638)
R_{work}† (%)	20.1 (27.4)
R_{free}‡ (%)	25.2 (33.1)
R.m.s.d. bonds (Å)/angles (°)	0.02/1.8
Dihedral angles	
Most favored (%)	95.97
Allowed (%)	4.03
No. of atoms	
Protein	6598
Ligands	270
Solvent	1506
Average B factor (Å^2)	
Protein	30.18
Ligands	28.81
Solvent	48.48
PDB code	3w4u

† $R_{merge} = \sum_{hkl}\sum_i |I_i(hkl) - \langle I(hkl)\rangle| / \sum_{hkl}\sum_i I_i(hkl)$. ‡ R_{free} was calculated with 5% of reflections that were excluded throughout the refinement.

respectively) and relative insensitivity to 2,3-diphosphoglycerate (2,3-DPG) or other phosphates (He & Russell, 2004*b*). The structural studies of CO-ligated Hb $\zeta_2\beta_2^s$ that we describe fully account for these unusual O_2-binding, cooperativity and allosteric properties. In addition, our results are singular in describing a unique heterotetramer that is trapped in the quaternary T conformation despite being fully liganded, making it the first such structure to be reported for mammalian hemoglobin from a liganded hemoglobin solution.

2. Experimental procedures

2.1. Protein production and purification

Human $\zeta_2\beta_2^s$ was obtained from complex transgenic knockout animals bred from parental mouse lines expressing 100% human Hb S ($\alpha_2\beta_2^s$; Pászty *et al.*, 1997) and full-length human ζ globin (Liebhaber & Russell, 1998), respectively, using a multi-generation mating strategy. The index mice expressed human ζ, α and β^s globins in the absence of endogenous adult mouse globins (He & Russell, 2004*a*,*b*; Liebhaber & Russell, 1998), producing a mixture of human Hb $\alpha_2\beta_2^s$ and Hb $\zeta_2\beta_2^s$ heterotetramers. The constituent transgenic globins are full length without epitope tags and appear to have undergone normal removal of their N-terminal methionine (not shown). Hb $\zeta_2\beta_2^s$ was purified from PBS-washed mouse erythrocytes saturated with CO and was stored at 193 K prior to use. Lysate was prepared in excess buffer *A* (40 m*M* bis-tris pH 6.5, 5 m*M* EDTA) and clarified by ultracentrifugation at ∼62 000*g* at 293 K for 20 min. Hemolysates were fractionated over an SP/H 4.5 × 100 Poros column (PerSeptive Biosystems, Foster City, California, USA) using a BioCAD Sprint perfusion chromatography system (Framingham, Massachusetts, USA). Hemoglobins were eluted at 2 ml min^{-1} using a 30–70% buffer *B* (buffer *A* + 200 m*M* NaCl) gradient and fractions were collected and analyzed as described previously (He & Russell, 2004*a*,*b*).

2.2. Crystallization, data collection and data processing

CO-liganded Hb $\zeta_2\beta_2^s$ was prepared by saturating the Hb with CO and sodium dithionite as previously reported (Safo & Abraham, 2005; Kidd *et al.*, 2001). Room-temperature crystallization was carried out by hanging-drop vapor diffusion using a solution consisting of 30 mg ml^{-1} protein and 3.2 *M* sodium/potassium phosphate pH 6.0. Prior to use, the crystals were washed in a cryoprotectant solution containing mother liquor and glycerol and were then flash-cooled. X-ray diffraction data were collected at 100 K with a Saturn92 CCD detector using Cu $K\alpha$ X-rays (λ = 1.54 Å) from an RU-H3R X-ray source with Osmic mirrors (Rigaku, The Woodlands, Texas, USA). The crystal diffracted to 1.95 Å resolution. The data were processed with the *d*TREK* software (Rigaku) and the *CCP*4 suite of programs (Winn *et al.*, 2011). The X-ray data are summarized in Table 1.

2.3. Structure determination and refinement

The systematic absences of (00*l*) reflections along the *c* axis indicated that the Hb $\zeta_2\beta_2^s$ crystal belonged to either space group $P3_121$ or $P3_221$. The structure was subsequently determined by the molecular-replacement method with *CNS* (Brünger *et al.*, 1998) using chimeric human ζ/mouse β heterotetrameric Hb ($\zeta_2^h\beta_2^m$) from PDB entry 1jeb as a search model (Kidd *et al.*, 2001). The Matthews coefficient predicted three dimers per asymmetric unit with a reasonable solvent content of ∼50%; a single distinct peak was observed in the cross-rotation function map, suggesting near-identical orientations of constituent dimers within the unit cell. A subsequent translational search in $P3_121$ yielded a three-dimer solution that gave an *R* value of 0.45 for all data from 19.95 to 1.95 Å resolution. Searches using the human $\alpha1\beta1$ dimer from PDB entry 1lw5 (Safo *et al.*, 2002) produced similar results.

Crystallographic symmetry operations indicated a tetramer comprising two dimers with constituent chains that we denote *A*, *B*, *C* and *D*. A third dimer (*E* and *F* chains) formed a tetramer with its dyad equivalent. The *A*, *C* and *E* chains correspond to ζ globin, while the *B*, *D* and *F* chains correspond to β^s globin. The initial difference Fourier map, calculated with an overall figure of merit (FOM) of 0.51, displayed well correlated electron densities for the six polypeptide chains and their corresponding heme groups. The model obtained from molecular replacement was manually adjusted using the program *Coot* (Emsley *et al.*, 2010). For the correct amino-acid sequence of Hb $\zeta_2\beta_2^s$, the *B*, *D* and *F* chains of $\zeta_2^h\beta_2^m$ were each replaced by a copy of the human β^s chain that contained the defining Glu→Val substitution at β-globin position 6. Four C-terminal residues in the *A* and *C* chains

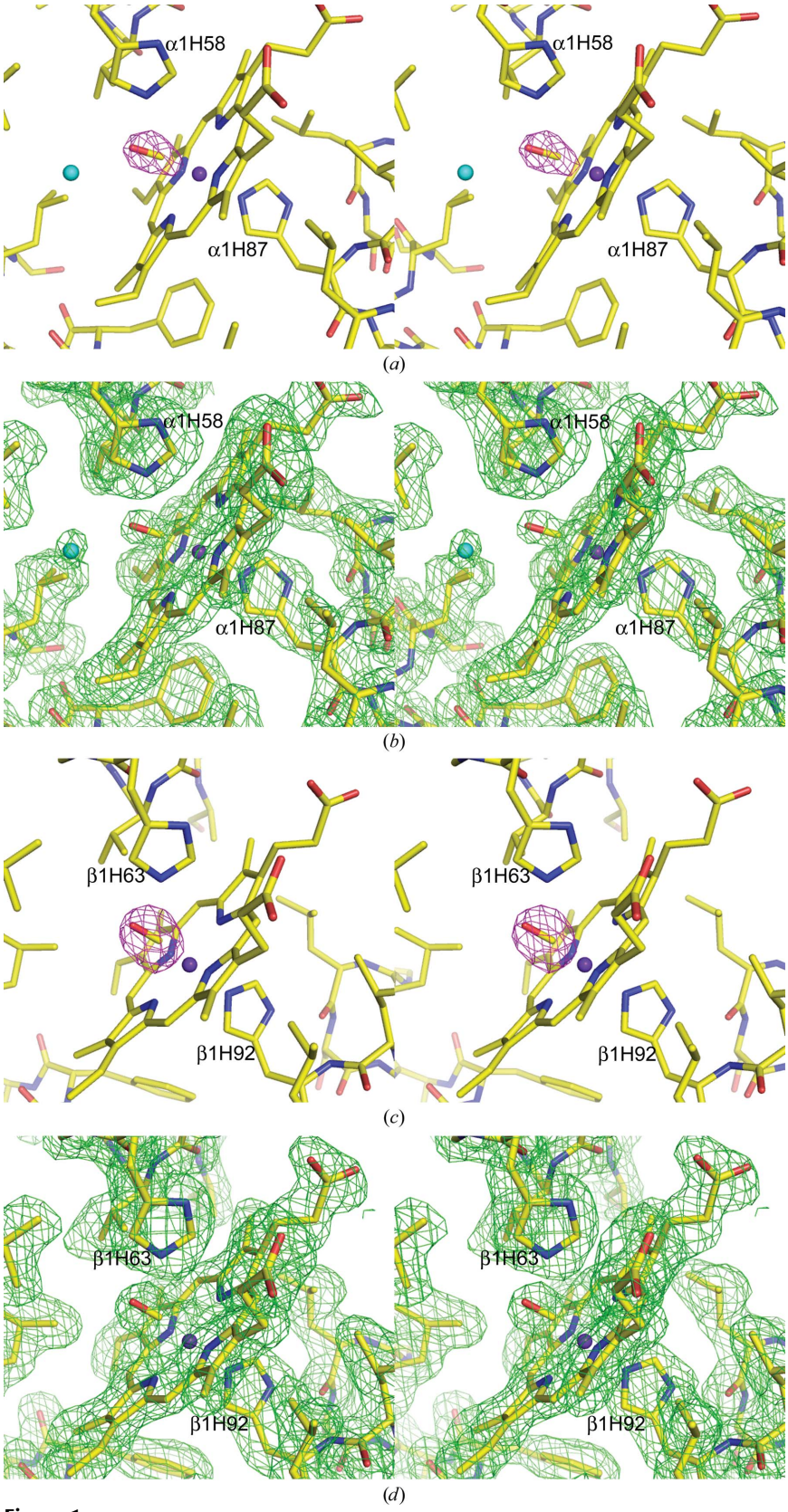

Figure 1
Stereoviews of the electron-density map and the final model of the Hb $\zeta_2\beta_2^s$ *ABCD* heme environment. (*a*) Composite $F_o - F_c$ OMIT map of the bound CO ligand at the ζ1 heme contoured at 5σ. (*b*) Final $2F_o - F_c$ map of the ζ1 heme and surrounding residues contoured at 1.2σ. (*c*) Composite $F_o - F_c$ OMIT map of the bound CO ligand at the β_s1 heme contoured at 5σ. (*d*) Final $2F_o - F_c$ map of the β_s1 heme and surrounding residues contoured at 1.2σ.

were refitted according to conformational changes. After preliminary refinement using *CNS*, the model yielded R and R_{free} values of 27 and 30%, respectively. Space group $P3_221$ also resulted in a similar three-dimer solution, with an R and an FOM of 47% and 0.48, respectively. The map also matched the protein model well, but after refinement the R and R_{free} values could only be reduced to 36 and 40%, respectively. A check of the data for possible twinning was negative. Consequently, the correct space group of this trigonal crystal is $P3_121$ (not $P3_221$). Moderate noncrystallographic symmetry restraints were imposed on equivalent chains throughout the refinement, in which simulated annealing was also employed. The criteria for adding water molecules were a higher level than 1.2σ in the $2F_o - F_c$ map and a closer distance than 8.0 Å from the protein. The final R and R_{free} values are 20.1 and 25.2%, respectively. Other statistics of the refined structure can be found in Table 1. Atomic coordinates and structure factors have been deposited in the PDB with accession code 3w4u.

3. Results

3.1. Overall structure

We have crystallized the CO-ligated Hb $\zeta_2\beta_2^s$ in space group $P3_121$, with unit-cell parameters $a = b = 115.5$, $c = 140.9$ Å. The diffraction data, refinement (1.95 Å) and structural statistics of Hb $\zeta_2\beta_2^s$ are summarized in Table 1. The asymmetric unit contains three heterodimers, two of which form a heterotetramer (denoted *ABCD*). A second heterotetramer (*EFGH*) can be generated from the remaining asymmetric heterodimer (*EF*) by the application of symmetry operators. The *A*, *C*, *E* and *G* subunits correspond to ζ-globin chains (amino acids 1–141), while the *B*, *D*, *F* and *H* subunits correspond to β^s-globin chains (amino acids 1–146). The root-mean-square deviation (r.m.s.d.) values among the four heterodimers (*AB*, *CD*, *EF* and *GH*) after least-squares superpositions of their constituent subunits were each ∼0.3 Å, while the r.m.s.d. between the two heterotetramers (*ABCD* and *EFGH*) was 0.5 Å, suggesting tertiary and quaternary structures that are highly similar. The three C-terminal ζ-chain residues (ζLys139, ζTyr140 and ζArg141) in the *EFGH* tetramer could not be resolved

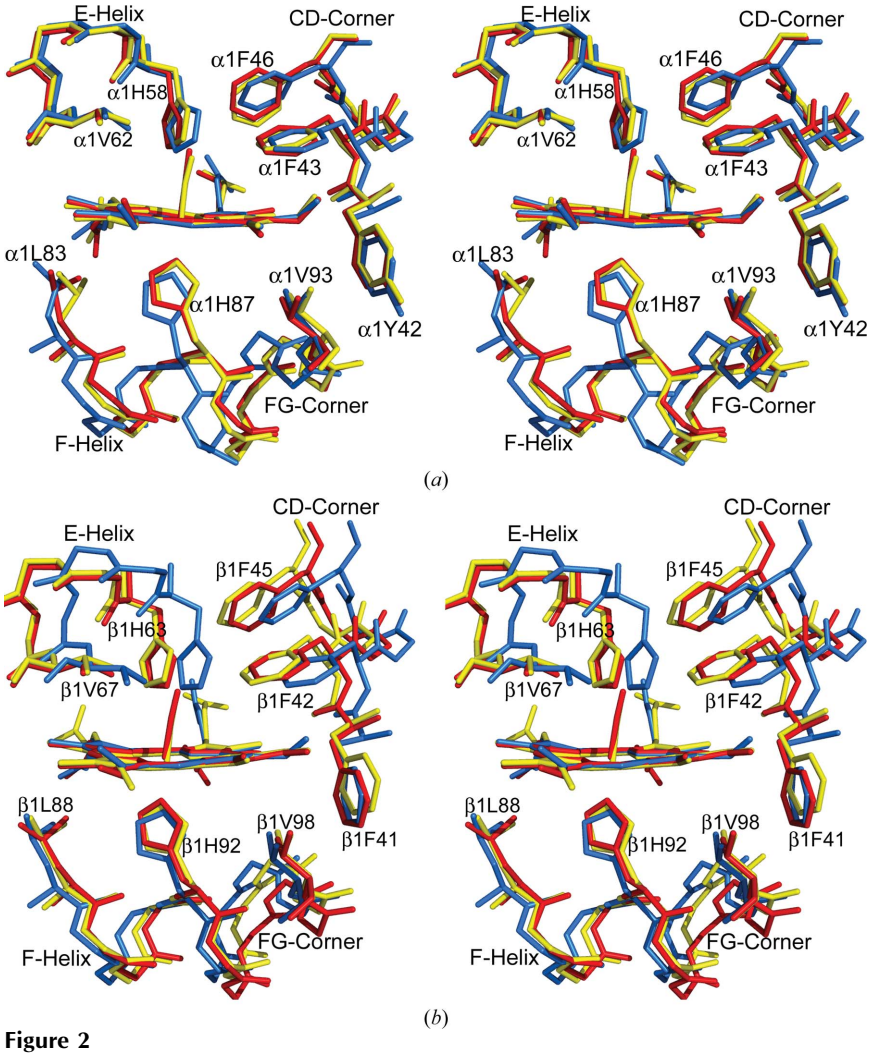

Figure 2
Stereoview of the heme environment of deoxy T (PDB entries 2hhb or 2dn2; cyan), CO-ligated R (PDB entries 1aj9 or 1ljw; red) and CO-ligated Hb $\zeta_2\beta^s_2$ (yellow) structures after superposing the $\alpha1$ ($\zeta1$) subunit or $\beta1$ subunit by least-squares fitting of the porphyrin pyrrole atoms. Note the different positions of the F helix, E helix, EF corner and CD corner. (*a*) The $\alpha1$ ($\zeta1$) heme. (*b*) The $\beta1$ heme (β^s1).

owing to disorder, while these same residues in the *ABCD* tetramer could be resolved but displayed signs of structural flexibility, especially in the $\zeta1$ subunit. The N-terminal β^sVal1 was absent from all β^s-chain residues owing to weak density.

Although the human ζ-globin and α-globin chains differ at 58 (of 141) amino-acid positions, least-squares superpositions of the liganded $\zeta1\beta^s1$ dimer on either T-state $\alpha1\beta1$ (deoxyHb A; PDB entries 2hhb and 2dn2; Fermi *et al.*, 1984; Park *et al.*, 2006) or R-state $\alpha1\beta1$ (COHb A; PDB entries 1aj9 and 1ljw; Vásquez *et al.*, 1998; Safo *et al.*, 2002) resulted in r.m.s.d. values of ∼0.7 Å, suggesting similar overall structures despite the significant differences at the C-termini of the constituent α-globin and ζ-globin chains. Previous comparisons of Hb quaternary structures reported similar r.m.s.d. values for $\alpha1\beta1$ or equivalent heterodimers (Jenkins *et al.*, 2009; Safo & Abraham, 2005), consistent with the fact that, unlike $\alpha1\beta2$, $\alpha1\alpha2$ and $\beta1\beta2$ dimers, the conformation of the $\alpha1\beta1$ dimer is largely indifferent to the allosteric state of the hetero-tetrameric structure.

31 of the 58 non-identical $\alpha\rightarrow\zeta$ residues are located on the surface of Hb $\zeta_2\beta^s_2$; most of these face the bulk solvent, while a smaller number of (mostly hydrophilic) residues participate in internal ζ-subunit hydrogen bonds. 21 of the nonconserved residues that are partially or fully buried within the ζ subunit are involved in hydrophobic interactions; three additional residues are positioned at the $\zeta1$–β^s1 interface (αPhe36$\rightarrow\zeta$His36, αPro119$\rightarrow\zeta$Ala119 and αAla120$\rightarrow\zeta$Glu120) but do not participate in hydrophobic or hydrogen-bond contacts or contribute to any significant structural changes in this region. Two residues, αVal131$\rightarrow\zeta$Ser131 and αSer134$\rightarrow\zeta$Thr134, are located at the $\zeta1$–$\zeta2$ interface but are not involved in direct intersubunit contacts in either Hb A or Hb $\zeta_2\beta^s_2$. Lastly, one residue (αThr38$\rightarrow\zeta$Gln38) is located at the $\zeta1$–β^s2 interface, where it participates in several water-mediated intersubunit interactions. The solvent-accessible surface area of the $\zeta1$–β^s1 interface was 855 Å^2, intermediate between the values of 832 and 873 Å^2 for the $\alpha1$–$\beta1$ interfaces of T-state and R-state structures of Hb A, respectively.

3.2. Heme cavity and dimer interface

The $\alpha\rightarrow\zeta$ exchange in Hb S effects only minor differences in the positioning of the liganded heme iron within the O_2-binding pocket. Each of the four ferrous ions in Hb $\zeta_2\beta^s_2$ is centered in the porphyrin plane, consistent with hexacoordination to residues of the encompassing globin subunit and to bound CO (Fig. 1), although the β^s2 heme of the *ABCD* tetramer appears to be slightly less occupied with CO than the remaining hemes. The stereochemistry of the Hb $\zeta_2\beta^s_2$-bound CO is similar to that observed for the R-state structure of COHb A (PDB entry 1ljw) except for a significant shortening of the hydrogen-bond interaction between the CO and the imidazole of the distal histidine (ζHis58 or β^sHis63) that stabilizes the bound ligand (2.4–2.8 Å *versus* ∼3.0 Å for R-structured Hb A).

In contrast, we noted subtle but significant tertiary structural changes in the heme environments of both the ζ and the β^s subunits, as well as in the $\zeta1$–β^s2 interfaces, when we superposed Hb $\zeta_2\beta^s_2$ on the porphyrin pyrrole atoms of both unliganded (PDB entries 2hhb and 2dn2) and liganded (PDB entries 1aj9 and 1ljw) Hb A structures (Fig. 2). In liganded Hb $\zeta_2\beta^s_2$, the E helix of the β^s subunit (and to a lesser extent the E helix of the ζ subunit), including the βVal67 and βHis63 side chains that sterically hinder β-subunit ligand binding in the T structure of Hb A, is moved in the direction of the R structure, effectively expanding the size of the distal heme

pocket. In addition, the FG corners of both the ζ and β^{s} subunits move to positions intermediate between the T and R positions described for Hb A, while the CD corners of the two subunits each advance past their positions in R-state Hb A, especially within the *ABCD* tetramer. In contrast to the CD and FG corners, other structural determinants of the $\zeta1$–$\beta^{s}2$ interface, including the ζ-subunit C helix and the β^{s} subunit F helix, move in an opposite direction beyond their classical positions in T-state Hb A, defining a highly unusual dimer interface that may account for the discordance between the function of the Hb $\zeta_2\beta_2^{s}$ heterotetramer and its ligand binding-site occupancy.

3.3. Quaternary structure

Liganded Hb $\zeta_2\beta_2^{s}$ crystallizes with a unique quaternary structure that is distinct in several important ways from the structures of both T-state and R-state Hb A. When superposed on reference T-state structures (PDB entries 2hhb and 2dn2), the Hb $\zeta_2\beta_2^{s}$ *ABCD* and *EFGH* tetramers exhibit high r.m.s.d. values of 1.7 and 1.9 Å, respectively, signaling significant structural dissimilarity. A similar comparison of Hb $\zeta_2\beta_2^{s}$ with reference R-state Hb A (PDB entries 1aj9 and 1ljw) yielded an even more significant r.m.s.d. value of 2.7 Å, a difference that exceeds the r.m.s.d. value of 2.1 Å that we observe when comparing the reference T-state and R-state structures of Hb A.

The significance of the quaternary-structural differences between liganded Hb $\zeta_2\beta_2^{s}$ and both unliganded and liganded Hb A was also apparent when we superposed the $\zeta1\beta^{s}1$ dimer of the *ABCD* tetramer on the $\alpha1\beta1$ dimer of the reference T-state or R-state Hb A and then calculated the angle of rotation required to superpose the corresponding, but non-aligned, $\zeta2\beta^{s}2$ and $\alpha2\beta2$ dimers. This process required rotations of 11.5 and 20.0°, respectively; by comparison, a rotation of 14° is required to superpose the $\alpha2\beta2$ dimers of the reference T and R structures of Hb A. Parallel analysis of the Hb $\zeta_2\beta_2^{s}$ *EFGH* tetramer required similar angles of rotation (13.2 and 21.1°) to permit superposition with reference T and R structures, respectively. Fig. 3(*a*) illustrates the positions of the non-aligned $\zeta2\beta^{s}2$ and $\alpha2\beta2$ dimers of the Hb $\zeta_2\beta_2^{s}$ T and R structures.

A more detailed analysis of specific structural markers places the quaternary structure of liganded Hb $\zeta_2\beta_2^{s}$ even closer to T-state Hb A than might be inferred from the r.m.s.d. values and angles of rotation that we observe. For example, at the $\zeta1\beta^{s}2$ dimer interface the β^{s}-globin FG corner residue (β^{S}2His97) is positioned between the CD corner residues ζ1Pro44 and ζ1Thr41, corresponding to its location in the T

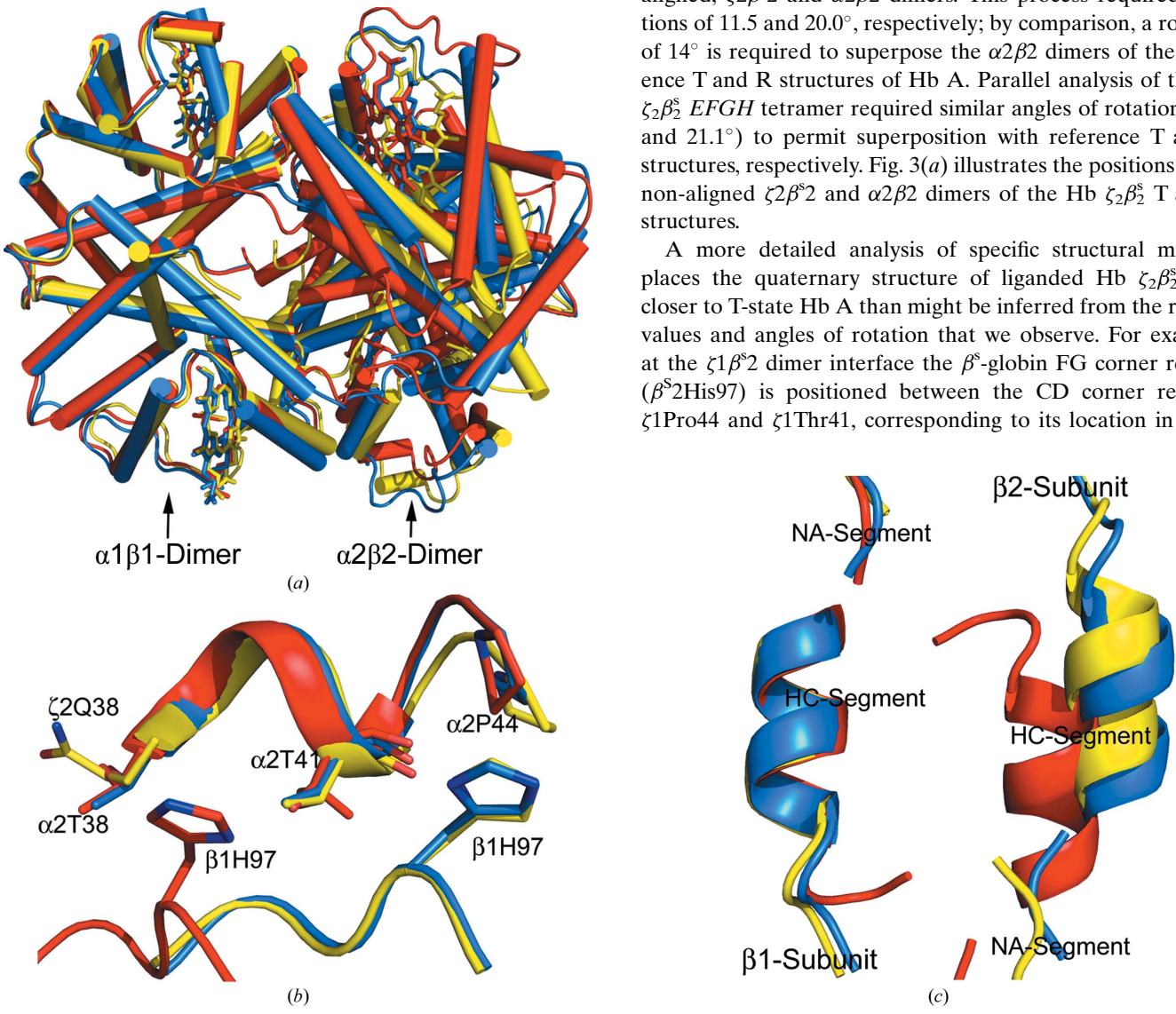

Figure 3
Quaternary-structural features of deoxy T (PDB entries 2hhb or 2dn2; cyan), CO-ligated R (PDB entries 1aj9 or 1ljw; red) and CO-ligated Hb $\zeta_2\beta_2^{s}$ (yellow) structures. The structures were each superposed on the main-chain atoms of the invariant $\alpha1\beta1$ and $\zeta1\beta^{s}1$ heterodimers. (*a*) Structural differences in the positions of the non-superposed $\alpha2\beta2$ and $\zeta2\beta^{s}2$ heterodimers. (*b*) The $\alpha1$–$\beta2$ ($\zeta1$–$\beta^{s}2$) interface showing the relative positions of the CD and FG corners. (*c*) The β-cleft.

Table 2
Hydrogen-bond interactions (in Å) in the T (PDB entry 2hhb), R (PDB entry 1aj9) and Hb $\zeta_2\beta_2^s$ structures.

In structures with a tetramer in the asymmetric unit, the contact distances shown are between the $\alpha1$–$\beta2$ ($\zeta1$–β^s2) interface or $\beta1$–$\beta1$ or $\alpha1$–$\alpha1$ ($\zeta1$–$\zeta2$). Corresponding contact distances were also observed at the symmetry-related dimer interfaces. Similar contact interactions were also obtained when PDB entries 2dn2 (T structure) or 1ljw (R structure) were used in the analysis.

				Hb $\zeta_2\beta_2^s$	
Contact		T	R	*ABCD*	*EFGH*
$\alpha1$Thr38 OH	$\beta2$His97 O	—	2.4	—	—
$\alpha1$Thr41 OH	$\beta2$His97 ND1	—	—	—	—
$\alpha1$Thr38 OH	$\beta2$Asp99 OD1	—	—	—	—
$\alpha1$Tyr42 OH	$\beta2$Asp99 OD1	2.5	—	2.4	2.4
$\alpha1$Asp94 OD2	$\beta2$Asn102 ND2	—	3.2	—	—
$\alpha1$Asn97 ND2	$\beta2$Asp99 OD1	2.8	—	2.9	2.8
$\alpha1$Leu91/Ile90 O	$\beta2$Arg40 NE	2.8	—	3.4	2.8
$\alpha1$Arg92 O	$\beta2$Arg40 NE	3.3	—	—	—
$\alpha1$Asp94 OD1	$\beta2$Trp37 NE1	3.0	3.3	—	—
$\beta1$His146 NE	$\beta1$Asp94 OD	2.8	—	2.7	2.6
$\beta1$His146 OT	$\alpha2$Lys40 NZ	2.5	—	2.7	2.7
$\alpha1$Arg141 NH2	$\alpha2$Asp126 OE	2.7	—	—	—
$\alpha1$Arg141 OT	$\alpha2$Lys127 NZ	2.8	—	—	—
$\alpha1$Tyr140 OH	$\alpha1$Val93 O	2.7	2.8	—	—
$\alpha1$Arg141 NH	$\beta2$Trp37 NE	—	—	3.3	Disorder
$\alpha1$Arg141 NH	$\alpha1$Arg92 O	—	—	3.4	Disorder
$\alpha1$Arg141 NH	$\alpha1$Asp94 OD	—	—	3.7	Disorder
$\alpha1$Glu138 OE1	$\alpha1$Arg92 NH2	—	—	3.2	Disorder

structure of Hb A and contrasting with its positioning between $\alpha1$Thr41 and $\alpha1$Thr38 in the liganded R structure of Hb A (Fig. 3*b*). The inferred absence of ligand-induced dimer-interface sliding in Hb $\zeta_2\beta_2^s$ has apparently led to the conservation of several interdimer salt-bridge/hydrogen-bond interactions that are characteristic of classical T-state quaternary structures [Table 2; $\zeta1$Tyr42–β^s2Asp99, $\zeta1$Asn97–β^s2Asp99, $\zeta1$Ile90–β^s2Arg40 ($\alpha1$Leu91–$\beta2$Arg40 in Hb A) and $\zeta1$Lys40–β^s2His146]. The integrities of these interactions are remarkable for a liganded hemoglobin and testify to the highly unusual structure (and corresponding function) of Hb $\zeta_2\beta_2^s$.

The T-like quaternary structure of Hb $\zeta_2\beta_2^s$ is also indicated by a separate measure of monomer–monomer positioning as reflected by the intersubunit iron–iron distance. The values for $\alpha1$–$\beta2$, $\alpha1$–$\alpha2$ and $\beta1$–$\beta2$ iron–iron distances in liganded Hb $\zeta_2\beta_2^s$ and unliganded T-state Hb A are highly similar, although both differ from R-state Hb (Table 3), consistent with other features of Hb $\zeta_2\beta_2^s$, indicating that this unusual hetero-tetramer maintains a T-state structure despite full ligation.

During the T-to-R-state transition of Hb A, the sliding motion of the $\alpha1\beta1$ dimer relative to the $\alpha2\beta2$ dimer also significantly alters both the size and the geometry of the central water cavity, as well as structural features that define both the α-cleft and the β-cleft. For instance, structures that delineate the central water cavity (EF corner–F helix), the α-cleft (NA and HC segments) and the β-cleft (NA segment, C helix–HC segment) move toward their symmetry-related counterparts in R-state Hb A, reducing the sizes of all three structural features (Jenkins *et al.*, 2009; Safo & Abraham, 2005). The apparent lack of interface sliding in liganded Hb $\zeta_2\beta_2^s$ predicts the larger central water cavity and intersubunit

Table 3
Iron–iron distances (in Å) in the T (PDB entry 2hhb), R (PDB entry 1aj9) and Hb $\zeta_2\beta_2^s$ structures.

In structures with a tetramer in the asymmetric unit, the distance is the average between two symmetry-related dimers. Similar distances were also obtained when PDB entries 2dn2 (T structure) or 1ljw (R structure) were used in the analysis.

Hemoglobin	$\alpha1\beta1$	$\alpha1\beta2$	$\alpha1\alpha2$	$\beta1\beta2$	Total
T	36.5	24.4	34.2	39.5	134.6
R	34.8	25.7	34.8	34.7	130.0
Hb $\zeta_2\beta_2^s$, *ABCD*	34.9	24.6	34.1	38.7	132.6
Hb $\zeta_2\beta_2^s$, *EFGH*	35.0	25.0	33.9	38.7	132.3

clefts that we observed in the crystal structure (Figs. 3*a* and 3*c*), which are similar to their sizes in unliganded Hb A. Collectively, these analyses demonstrate a quaternary structure for heterotetrameric Hb $\zeta_2\beta_2^s$ that, even though fully liganded, differs more substantially from liganded (R-state) Hb A than from unliganded (T-state) Hb A, suggesting unique structure–function properties that have not previously been described.

3.4. C-terminal interactions

Salt-bridge and/or hydrogen-bond interactions involving C-terminal residues of both the α and the β subunits of Hb A appear to be key determinants of its ligand affinity (Perutz *et al.*, 1993, 1994, 1998; Bettati *et al.*, 1997, 1998; Kavanaugh, Rogers & Arnone, 1992). In the reference T structure of Hb A, the $\alpha1$Arg141 carboxyl and guanidinium groups contribute to intersubunit salt bridges with $\alpha2$Lys127 and $\alpha2$Asp126, while the $\beta1$His146 carboxyl and imidazolium groups interact with $\alpha2$Lys40 and $\beta1$Asp94, respectively (Table 2). These interactions, which stabilize the T structure and decrease its affinity for O_2, are absent in liganded R-state Hb A. While the ζArg141-associated salt bridges appear to be ruptured in liganded Hb $\zeta_2\beta_2^s$, the corresponding interactions involving β^sHis146 are maintained (Table 2; Figs. 4*a* and 4*b*). These observations permit unique inferences about the importance of these interactions to the function of heterotetrameric hemoglobins, as well as clues to the temporal order in which the C-terminal interactions are disrupted during the T→R transition. As in the reference R-state Hb A, the ζ-chain C-terminus of the *EFGH* tetramer is highly mobile and cannot be fully resolved, while the corresponding region of the *ABCD* tetramer is largely fixed because of the interactions of $\zeta1$Arg141 with β^s2Trp37, $\zeta1$Asp94, $\zeta1$Arg92 and $\zeta1$Glu138 (Table 2; Fig. 4*c*). This observation may capture or reflect subtle structural changes that accompany ligand binding and may partly explain why two independent Hb molecules are observed in the asymmetric unit.

4. Discussion

4.1. Liganded Hb $\zeta_2\beta_2^s$ is trapped in a quaternary T-state-like conformation

Our structural analyses characterize a functional variant human hemoglobin comprising both embryonic and adult

globin subunits that is unique insofar as it exhibits a quaternary T-state-like structure even when fully liganded. Hb $\zeta_2\beta^s_2$ displays specific quaternary T-state features, including $\zeta1$–β^s2 interface packing of β^s2His97 (Fig. 3*b*), conserved $\zeta1$–β^s2, $\zeta1$–$\zeta2$ and β^s1–β^s2 intersubunit hydrogen-bond interactions (Table 2), preserved β^sHis146 salt-bridge interactions (Table 2, Fig. 4*a*), an enlarged central water cavity and β-cleft (Figs. 3*a* and 3*c*) and intersubunit iron–iron distances (Table 3). While they predominate, the T-state characteristics of Hb $\zeta_2\beta^s_2$ are not complete. Several high-affinity r features that are more commonly observed in quaternary R structures, including the positioning of the liganded Fe^{2+} within the porphyrin plane, the enlargement of the heme distal pockets by displacement of the E helix (Fig. 2) and the movement of the CD and FG corners toward the central water cavity (Fig. 2), are found in Hb $\zeta_2\beta^s_2$ and may partly account for the high ligand affinity of Hb $\zeta_2\beta^s_2$ in the context of a T-state-like quaternary structure.

The discovery of a previously unknown relaxed (R2) structure from a crystal grown under near-physiological low-salt conditions (Silva *et al.*, 1992) initiated a controversy regarding the physiological relevance of the classical relaxed (R) structure, which had been crystallized under high-salt conditions. Such effects, if they exist, are unlikely to have contributed to the T-state structure that we observe for Hb $\zeta_2\beta^s_2$. When crystallized in high-salt solutions similar to those that we employ, liganded Hb A invariably displays a quaternary relaxed structure (*e.g.* R, RR2, R2 or R3) (Safo *et al.*, 2004, 2011; Jenkins *et al.*, 2009; Safo & Abraham, 2005; Mueser *et al.*, 2000; Silva *et al.*, 1992; Schumacher *et al.*, 1995, 1997; Janin & Wodak, 1993), in contrast to the quaternary tense structure described here. Moreover, a number of different relaxed structures can be obtained for heterologous hemoglobins using high-salt methods and in some instances using both high-salt and low-salt conditions (Safo *et al.*, 2004, 2011; Jenkins *et al.*, 2009; Safo & Abraham, 2005; Mueser *et al.*, 2000; Silva *et al.*, 1992; Schumacher *et al.*, 1995, 1997; Janin & Wodak, 1993; Bhatt *et al.*, 2011), consistent with NMR evidence that the various relaxed structures, including the classical R structure, exist in nature in an ensemble of states (Lukin *et al.*, 2003), and that Hb function involves such an ensemble of relaxed hemoglobin states in dynamic equilibrium (Safo *et al.*, 2011; Jenkins *et al.*, 2009; Safo & Abraham, 2005). These observations indicate that the high-

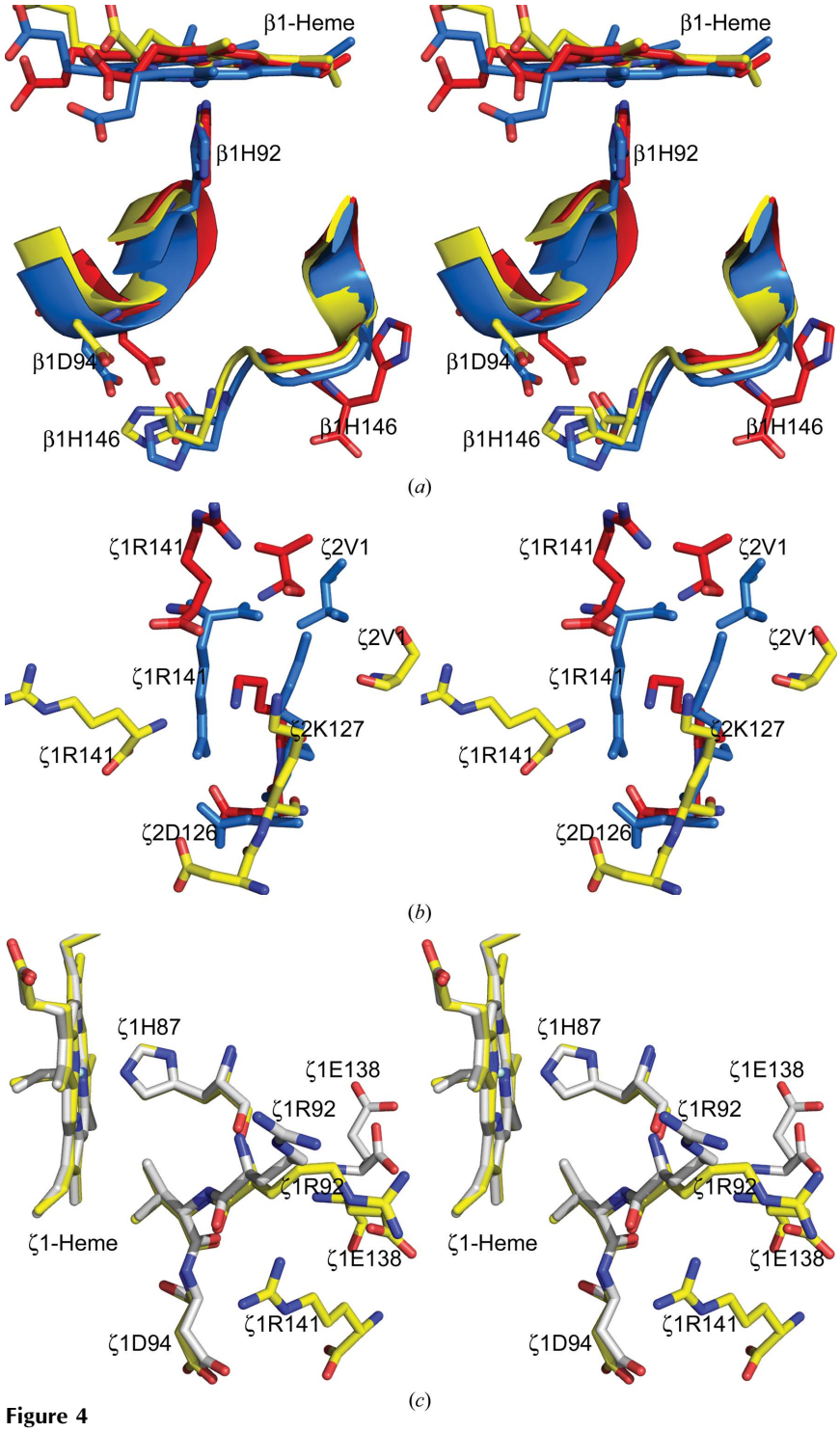

Figure 4
Stereoview of interactions associated with the α- (ζ-) and β-subunit C-termini in the T (PDB entries 2hhb or 2dn2; cyan), R (PDB entries 1aj9 or 1ljw; red), Hb $\zeta_2\beta^s_2$ *ABCD* (yellow) and/or *EFGH* (gray) structures. (*a*) The T-state salt-bridge interaction between β1His146 and β1Asp94 is broken in the R structure but is maintained in the liganded Hb $\zeta_2\beta^s_2$ structure. (*b*) The T-state salt-bridge interactions between α1Arg141 and α2Lys120 and α2Asp126 are broken in both the R and the liganded Hb $\zeta_2\beta^s_2$ structures. (*c*) Reorientation of the Hb $\zeta_2\beta^s_2$ *ABCD* ζ-subunit C-terminus results in hydrogen-bond interactions between ζ1Arg141 and the F-helix residues ζ1Arg92, ζ1Asp94 and ζ1Glu138. The corresponding interactions in the *EFGH* tetramer are missing owing to disorder of the ζArg141 residue.

salt crystallization conditions used here are unlikely to have artifactually trapped liganded Hb $\zeta_2\beta^s_2$ in the quaternary T structure.

To our knowledge, this is the first reported example of a fully liganded mammalian hemoglobin crystallized from a CO-saturated solution that remains trapped in a quaternary T-state-like conformation. Liganded hemoglobins naturally assume a quaternary relaxed conformation under these experimental conditions; liganded T-state structures can be generated, but only by exposing unliganded deoxyHb A crystals to either air or CO. Even under these conditions, the crystal has either to be grown in a concentrated PEG solution, frozen or stabilized with an allosteric effector prior to ligand exposure to prevent hemoglobin transition to an R-state structure that would crack or melt the crystal (Paoli *et al.*, 1996, 1997; Mozzarelli *et al.*, 1997; Abraham *et al.*, 1992; Rivetti *et al.*, 1993). These 'constrained' liganded T-state hemoglobins maintain the high-affinity r features, both in the heme pockets and in subunit-interface interactions, that we observe in liganded Hb $\zeta_2\beta^s_2$, validating this feature of its overall structure. Importantly, the magnitudes of the structural changes that we note for liganded Hb $\zeta_2\beta^s_2$ are significantly greater than those of constrained liganded T-state hemoglobins, consistent with cooperative events in liganded Hb $\zeta_2\beta^s_2$ in solution that are largely absent in liganded heterotetramers that are experimentally constrained to a T-state structure (Mozzarelli *et al.*, 1991, 1997; Bettati *et al.*, 1996; Rivetti *et al.*, 1993).

The quaternary T-state structural characteristics of Hb $\zeta_2\beta^s_2$ may be largely explained by the unusual positioning of the ζ-subunit CD corner residues (Pro37–Pro44) that mediate $\zeta1$–β^s2 interface sliding. In contrast to Hb A, which contains residues with short side chains (*e.g.* αPro37, αThr38, αThr41 and αPro44), Hb $\zeta_2\beta^s_2$ contains a long side chain at ζGln38 (Fig. 3*b*). The resulting steric constraint would be predicted to inhibit transitional interface sliding, promoting ligand binding to the Hb $\zeta_2\beta^s_2$ heterotetramer while it remains in a T-state structure. This hypothesis is consistent with the lowered subunit cooperativity that results from a ζ-for-α substitution in a number of other heterotetrameric hemoglobins, including human Hb $\alpha_2\beta_2$ (Kidd *et al.*, 2001; He & Russell, 2001) and a chimeric Hb $\alpha_2\beta_2$ containing murine β-globin subunits (Kidd *et al.*, 2001; He & Russell, 2000). These shared functional changes in the context of three different β-globin subunits, human β, human β^s and murine β, implicate structural differences between the human α-globin and ζ-globin subunits that are causal for these metrics. Moreover, the steric effect in each case is likely to be augmented by intersubunit interactions (*via* water mediation) between ζ1Gln38 and both β^s2Asp99 and β^s2Glu101 that stabilize the T-state structure and further restrain interface sliding during ligand binding.

4.2. Structural basis for Hb $\zeta_2\beta^s_2$ cooperativity

The structural analyses of Hb $\zeta_2\beta^s_2$ reported here provide important insights into the relatively low ligand-binding cooperativity that it exhibits (He & Russell, 2004*b*). In Hb A, the T$\rightarrow$R transition is characterized by a coordinated tertiary movement of the FG and CD corners of the α and β subunits, respectively, towards the $\alpha1$–$\beta2$ dimer interface, an action that is central to the cooperative nature of hemoglobin ligand binding (Perutz, 1972*b*; Perutz *et al.*, 1998; Paoli *et al.*, 1997; Baldwin & Chothia, 1979). Although the ζ and β^s subunits of Hb $\zeta_2\beta^s_2$ exhibit positioning of the FG and CD corners in the direction of an R-state structure, subunit sliding does not appear to occur, indicating that transition to the R state is not fully achieved. Differences in cooperativity between liganded Hb $\alpha_2\beta_2$ and unliganded Hb $\zeta_2\beta^s_2$ are likely to reflect subtle changes in the arrangement of their subunits, including the loss of salt-bridge interactions involving α1Arg141; nevertheless, steric restrictions to T$\rightarrow$R transition in Hb $\zeta_2\beta^s_2$ (and, specifically, steric constraint by the long side chain of ζGln38) implicate the activity of tertiary cooperativity events that occur within the T-like structure and are largely independent of quaternary effects. These observations are inconsistent with the MWC tenet that cooperative oxygen binding cannot occur in the absence of quaternary transition (Monod *et al.*, 1965), instead favoring the tertiary two-state and global allostery models (Henry *et al.*, 2002; Eaton *et al.*, 2007; Viappiani *et al.*, 2004; Yonetani *et al.*, 2002; Yonetani & Tsuneshige, 2003). Results from ongoing structural studies of deoxyHb $\zeta_2\beta^s_2$ and, specifically, confirmation of the prediction that it will display intact T-state α1Arg141 salt-bridge interactions will provide further insights into Hb $\zeta_2\beta^s_2$ cooperativity as well as the basis for its unusual allosteric properties.

4.3. Hb $\zeta_2\beta^s_2$ exhibits a high ligand affinity that is weakly affected by allosteric modifiers

The difference in the O_2 affinities of the T and R structures of Hb A ($\sim$14.7 kJ per mole of heme) has been attributed in part to the constraints imposed on the T structure by salt-bridge interactions between α1Arg141 and both α2Lys127 and α2Asp126 (Imai, 1982), a conclusion that is supported by several independent lines of evidence. Structural perturbations that either weaken or abolish these interactions are permissive for ligand-induced alterations to the quaternary structure that act to increase ligand affinity (Rivetti *et al.*, 1993; Luisi *et al.*, 1990). The experimental deletion of αArg141 (des-αArg141) produces a variant hemoglobin that displays a 15-fold increase in O_2 affinity (Kavanaugh *et al.*, 1995), while a naturally occurring β-chain mutation ($\beta^{\rm Rothschild}$; βTrp37Arg) that increases the positional mobility of αArg141 assembles a heterotetramer that exhibits a corresponding tenfold increase in this metric (Kavanaugh, Rogers, Case *et al.*, 1992; Rivetti *et al.*, 1993; Liddington *et al.*, 1988). The high ligand-binding affinity of Hb $\zeta_2\beta^s_2$, which contains a highly flexible C-terminus, may result from a similar weakening of ζArg141 salt-bridge interactions. This mechanism is unlikely to be fully explained by quaternary effects, as the crystal structure reveals a heterotetramer that binds gaseous ligands in solution but fails to transition from a quaternary T form to a corresponding R form. This observation is inconsistent with allosteric models that strictly couple ligand binding to quaternary transition

(Perutz *et al.*, 1998; Monod *et al.*, 1965), according instead with a tertiary two-state allosteric model of quaternary T and R states that are each populated by high-affinity and low-affinity r and t conformations, respectively (Henry *et al.*, 2002; Eaton *et al.*, 2007; Viappiani *et al.*, 2004). While we cannot strictly exclude the contribution of subtle quaternary changes to this effect (above), the high-affinity r conformation that we observe for Hb $\zeta_2\beta^s_2$, within the quaternary T state is, nevertheless, consistent with this latter model, as its reactivity with ligand is largely independent of any pronounced allosteric transition.

Our structural analyses do not exclude the possibility that differences in ligand-binding affinity may result in part from amino-acid differences between α and ζ globin at any of several other positions. We note, for example, the change from Pro to Ala at position 119 of the ζ-globin chain would be predicted to weaken hydrophobic interactions with β^sMet55 at the $\alpha1\beta^s1$ interface and to consequently destabilize the T state (Bhatt *et al.*, 2011), consistent with the effect of a similar amino-acid substitution on the O_2 affinity of the hemoglobin expressed by bar-headed geese (Zhang *et al.*, 1996). Additional studies will certainly be required to fully account for the relative contribution of this and other candidate amino-acid differences to the ligand-binding affinities of heterotetramers containing ζ-globin subunits.

The crystallographic result also accounts for the weak 2,3-DPG allostery that is experimentally observed for Hb $\zeta_2\beta^s_2$ (He & Russell, 2004*b*). 2,3-DPG plays a central role in hemoglobin allostery by preferentially binding to the enlarged T-state β-cleft, stabilizing the T structure and consequently reducing Hb–O_2 affinity. Fully liganded Hb $\zeta_2\beta^s_2$ displays an enlarged β-cleft that is characteristic of a T-state structure (Fig. 3*c*), predicting relatively little difference in the affinity of 2,3-DPG for unliganded or liganded Hb $\zeta_2\beta^s_2$ and suggesting a similarly modest effect on Hb $\zeta_2\beta^s_2$ O_2 affinity.

4.4. Hb $\zeta_2\beta^s_2$ exhibits a weak Bohr effect

Our crystal structure additionally accounts for the unusual pH allostery of Hb $\zeta_2\beta^s_2$. The Bohr effect has been attributed in part to heterotropic effects that are independent of quaternary transitions (Yonetani *et al.*, 2002; Yonetani & Tsuneshige, 2003; Shibayama & Saigo, 2001) and in part to the disruption of salt bridges that form in quaternary T structures and break in R structures, including β1His146 to β1Asp94 and α1Arg141 to both α2Lys127 and α2Asp126 (Perutz, 1976; O'Donnell *et al.*, 1979; Perutz *et al.*, 1994; Kavanaugh, Rogers, Case *et al.*, 1992; Kavanaugh *et al.*, 1995). Remarkably, fully liganded Hb $\zeta_2\beta^s_2$ maintains the βHis146–βAsp94 salt bridge, negating the contribution of this structure to the Bohr effect. The small pH effect that *is* observed for Hb $\zeta_2\beta^s_2$ is likely to result from labile ζArg141 salt-bridge interactions that are disrupted in T-state hemoglobin, as well as from secondary chloride-associated interactions involving ζVal1 that have been observed in other hemoglobins. Our observations that the liganded Hb $\zeta_2\beta^s_2$ maintains the β^sHis146 but not the ζArg141 salt bridges refine the current understanding of the Bohr effect mechanism (Bettati *et al.*, 1998; Perutz *et al.*, 1987; Bettati & Mozzarelli, 1997), both suggesting the order with which these critical interactions are disrupted during T→R transition and identifying the specific structure (the βHis146 salt bridge) that is most fundamental to this process. Consequently, this model emphasizes the mechanistic importance of αArg141 as a critical tertiary-structure determinant of the Hb Bohr effect and ligand affinity.

5. Conclusions

The current study reports new structural data for Hb $\zeta_2\beta^s_2$ that fully account for its unusual O_2-binding properties, including its high O_2 affinity, low cooperativity and reduced allosteric response to [H^+] and 2,3-DPG (He & Russell, 2004*b*). Moreover, the analyses demonstrate that ligand binding to Hb $\zeta_2\beta^s_2$ is effected less by the specific quaternary state than by tertiary-structural changes within the larger T- state or R-state structures. Our results accord with earlier work by several investigators, providing atomic-level insights into the contributions of tertiary and quaternary structures to cooperative Hb–O_2 ligand binding and validating the general principle that hemoglobin ligand affinity can be decoupled from overall quaternary structure (Yonetani *et al.*, 2002; Yonetani & Tsuneshige, 2003; Henry *et al.*, 2002). The *ABCD* and *EFGH* tetramers of Hb $\zeta_2\beta^s_2$ display significant tertiary conformational differences in the heme environment, ligand occupancy and dimer interface, despite their highly similar overall quaternary structure, suggesting that they represent discrete structural intermediates that exist during hemoglobin ligand binding. Studies of other heterotetrameric hemoglobins comprising developmental stage-discordant monomeric subunits (Hbs $\zeta_2\gamma_2$, $\zeta_2\beta_2$ and $\alpha_2\varepsilon_2$) may be highly informative in this regard.

We gratefully acknowledge research support from a VCU Presidential Research Initiative Program Award and an A. D. Williams Research Award (MKS), NIH grants HL061399 and HL082754 (JER), NIH grant HL103186 (OA) and NIH grant 5P20RR016439-05 (Joseph Bonaventura). Structural biology resources were provided in part by NIH grant CA16059 to the VCU Massey Cancer Center.

References

Abraham, D. J., Peascoe, R. A., Randad, R. S. & Panikker, J. (1992). *J. Mol. Biol.* **227**, 480–492.
Baldwin, J. & Chothia, C. (1979). *J. Mol. Biol.* **129**, 175–220.
Bettati, S., Kwiatkowski, L. D., Kavanaugh, J. S., Mozzarelli, A., Arnone, A., Rossi, G. L. & Noble, R. W. (1997). *J. Biol. Chem.* **272**, 33077–33084.
Bettati, S. & Mozzarelli, A. (1997). *J. Biol. Chem.* **272**, 32050–32055.
Bettati, S., Mozzarelli, A. & Perutz, M. F. (1998). *J. Mol. Biol.* **281**, 581–585.
Bettati, S., Mozzarelli, A., Rossi, G. L., Tsuneshige, A., Yonetani, T., Eaton, W. A. & Henry, E. R. (1996). *Proteins*, **25**, 425–437.
Bhatt, V. S., Zaldívar-López, S., Harris, D. R., Couto, C. G., Wang, P. G. & Palmer, A. F. (2011). *Acta Cryst.* D**67**, 395–402.
Brünger, A. T., Adams, P. D., Clore, G. M., DeLano, W. L., Gros, P., Grosse-Kunstleve, R. W., Jiang, J.-S., Kuszewski, J., Nilges, M.,

Pannu, N. S., Read, R. J., Rice, L. M., Simonson, T. & Warren, G. L. (1998). *Acta Cryst.* D**54**, 905–921.
Bruno, S., Bonaccio, M., Bettati, S., Rivetti, C., Viappiani, C., Abbruzzetti, S. & Mozzarelli, A. (2001). *Protein Sci.* **10**, 2401–2407.
Bunn, H. F. & Forget, B. G. (1986). *Hemoglobin: Molecular, Genetic and Clinical Aspects.* Philadelphia: W. B. Saunders.
Eaton, W. A., Henry, E. R., Hofrichter, J., Bettati, S., Viappiani, C. & Mozzarelli, A. (2007). *IUBMB Life*, **59**, 586–599.
Emsley, P., Lohkamp, B., Scott, W. G. & Cowtan, K. (2010). *Acta Cryst.* D**66**, 486–501.
Fermi, G. (1975). *J. Mol. Biol.* **97**, 237–256.
Fermi, G., Perutz, M. F., Shaanan, B. & Fourme, R. (1984). *J. Mol. Biol.* **175**, 159–174,
He, Z. & Russell, J. E. (2000). *Br. J. Haematol.* **108**, 430–433.
He, Z. & Russell, J. E. (2001). *Blood*, **97**, 1099–1105.
He, Z. & Russell, J. E. (2002). *Proc. Natl Acad. Sci. USA*, **99**, 10635–10640.
He, Z. & Russell, J. E. (2004*a*). *Nature Med.* **10**, 365–367.
He, Z. & Russell, J. E. (2004*b*). *Biochem. Biophys. Res. Commun.* **325**, 1376–1382.
Henry, E. R., Bettati, S., Hofrichter, J. & Eaton, W. A. (2002). *Biophys. Chem.* **98**, 149–164.
Imai, K. (1982). *Allosteric Effects in Haemoglobin.* Cambridge University Press.
Janin, J. & Wodak, S. J. (1993). *Proteins*, **15**, 1–4.
Jenkins, J. D., Musayev, F. N., Danso-Danquah, R., Abraham, D. J. & Safo, M. K. (2009). *Acta Cryst.* D**65**, 41–48.
Kavanaugh, J. S., Chafin, D. R., Arnone, A., Mozzarelli, A., Rivetti, C., Rossi, G. L., Kwiatkowski, L. D. & Noble, R. W. (1995). *J. Mol. Biol.* **248**, 136–150.
Kavanaugh, J. S., Rogers, P. H. & Arnone, A. (1992). *Biochemistry*, **31**, 8640–8647.
Kavanaugh, J. S., Rogers, P. H., Case, D. A. & Arnone, A. (1992). *Biochemistry*, **31**, 4111–4121.
Kidd, R. D., Russell, J. E., Watmough, N. J., Baker, E. N. & Brittain, T. (2001). *Biochemistry*, **40**, 15669–15675.
Lee, A. W. & Karplus, M. (1983). *Proc. Natl Acad. Sci. USA*, **80**, 7055–7059.
Liddington, R., Derewenda, Z., Dodson, G. & Harris, D. (1988). *Nature (London)*, **331**, 725–728.
Liebhaber, S. A. & Russell, J. E. (1998). *Ann. N. Y. Acad. Sci.* **850**, 54–63.
Luisi, B., Liddington, B., Fermi, G. & Shibayama, N. (1990). *J. Mol. Biol.* **214**, 7–14.
Lukin, J. A., Kontaxis, G., Simplaceanu, V., Yuan, Y., Bax, A. & Ho, C. (2003). *Proc. Natl Acad. Sci. USA*, **100**, 517–520.
Monod, J., Wyman, J. & Changeux, J.-P. (1965). *J. Mol. Biol.* **12**, 88–118.
Mozzarelli, A., Rivetti, C., Rossi, G. L., Eaton, W. A. & Henry, E. R. (1997). *Protein Sci.* **6**, 484–489.
Mozzarelli, A., Rivetti, C., Rossi, G. L., Henry, E. R. & Eaton, W. A. (1991). *Nature (London)*, **351**, 416–419.
Mueser, T. C., Rogers, P. H. & Arnone, A. (2000). *Biochemistry*, **39**, 15353–15364.
O'Donnell, S., Mandaro, R., Schuster, T. M. & Arnone, A. (1979). *J. Biol. Chem.* **254**, 12204–12208.
Paoli, M., Dodson, G., Liddington, R. C. & Wilkinson, A. J. (1997). *J. Mol. Biol.* **271**, 161–167.
Paoli, M., Liddington, R., Tame, J., Wilkinson, A. & Dodson, G. (1996). *J. Mol. Biol.* **256**, 775–792.
Park, S.-Y., Yokoyama, T., Shibayama, N., Shiro, Y. & Tame, J. R. H. (2006). *J. Mol. Biol.* **360**, 690–701.
Pászty, C., Brion, C. M., Manci, E., Witkowska, H. E., Stevens, M. E., Mohandas, N. & Rubin, E. M. (1997). *Science*, **278**, 876–878.
Perutz, M. F. (1972*a*). *Nature (London)*, **237**, 495–499.
Perutz, M. F. (1972*b*). *Biochimie*, **54**, 587–588.
Perutz, M. F. (1976). *Br. Med. Bull.* **32**, 195–208.
Perutz, M. F. (1989). *Q. Rev. Biophys.* **22**, 139–237.
Perutz, M. F., Fermi, G., Luisi, B., Shaanan, B. & Liddington, R. C. (1987). *Cold Spring Harb. Symp. Quant. Biol.* **52**, 555–565.
Perutz, M. F., Fermi, G., Poyart, C., Pagnier, J. & Kister, J. (1993). *J. Mol. Biol.* **233**, 536–545.
Perutz, M. F., Shih, D. T. & Williamson, D. (1994). *J. Mol. Biol.* **239**, 555–560.
Perutz, M. F., Wilkinson, A. J., Paoli, M. & Dodson, G. G. (1998). *Annu. Rev. Biophys. Biomol. Struct.* **27**, 1–34.
Rivetti, C., Mozzarelli, A., Rossi, G. L., Henry, E. R. & Eaton, W. A. (1993). *Biochemistry*, **32**, 2888–2906.
Safo, M. K., Abdulmalik, O., Danso-Danquah, R., Burnett, J. C., Nokuri, S., Joshi, G. S., Musayev, F. N., Asakura, T. & Abraham, D. J. (2004). *J. Med. Chem.* **47**, 4665–4676.
Safo, M. K. & Abraham, D. J. (2005). *Biochemistry*, **44**, 8347–8359.
Safo, M. K., Ahmed, M. H., Ghatge, M. S. & Boyiri, T. (2011). *Biochim. Biophys. Acta*, **1814**, 797–809.
Safo, M. K., Burnett, J. C., Musayev, F. N., Nokuri, S. & Abraham, D. J. (2002). *Acta Cryst.* D**58**, 2031–2037.
Schumacher, M. A., Dixon, M. M., Kluger, R., Jones, R. T. & Brennan, R. G. (1995). *Nature (London)*, **375**, 84–87.
Schumacher, M. A., Zheleznova, E. E., Poundstone, K. S., Kluger, R., Jones, R. T. & Brennan, R. G. (1997). *Proc. Natl Acad. Sci. USA*, **94**, 7841–7844.
Shibayama, N. & Saigo, S. (2001). *FEBS Lett.* **492**, 50–53.
Silva, M. M., Rogers, P. H. & Arnone, A. (1992). *J. Biol. Chem.* **267**, 17248–17256.
Szabo, A. & Karplus, M. (1972). *J. Mol. Biol.* **72**, 163–197.
Vásquez, G. B., Ji, X., Fronticelli, C. & Gilliland, G. L. (1998). *Acta Cryst.* D**54**, 355–366.
Viappiani, C., Bettati, S., Bruno, S., Ronda, L., Abbruzzetti, S., Mozzarelli, A. & Eaton, W. A. (2004). *Proc. Natl Acad. Sci. USA*, **101**, 14414–14419.
Winn, M. D. *et al.* (2011). *Acta Cryst.* D**67**, 235–242.
Yonetani, T., Park, S. I., Tsuneshige, A., Imai, K. & Kanaori, K. (2002). *J. Biol. Chem.* **277**, 34508–34520.
Yonetani, T. & Tsuneshige, A. (2003). *C. R. Biol.* **326**, 523–532.
Zhang, J., Hua, Z., Tame, J. R. H., Lu, G., Zhang, R. & Gu, X. (1996). *J. Mol. Biol.* **255**, 484–493.